Multimodality Imaging of Tumor Integrin $\alpha_v\beta_3$ Expression

Xiaoyuan Chen*

Molecular Imaging Program at Stanford (MIPS), Department of Radiology, Stanford University, Stanford, CA 94305, USA

Abstract: Most solid tumors are angiogenesis dependent. Anti-angiogenic pharmaceuticals that inhibit the growth of new blood vessels offer considerable promise as anti-cancer agents. With increasing numbers of anti-angiogenic drugs in clinical trials, there is an urgent need for detailed characterization of the heterogeneity of tumor vasculature and dissection of the complex network of mechanisms that control tumor angiogenesis. Non-invasive molecular imaging will play a key role in individualized anti-angiogenic therapy based upon molecular features of the new blood vessel growth. Integrin $\alpha_V\beta_3$, which binds several ligands via an RGD tripeptide sequence, is uniquely expressed in tumor vasculature and aggressive tumor cells, making it a potential target for anti-angiogenic interventions. This review highlights some recent advances in multimodality imaging of tumor integrin expression with emphasis on positron emission tomography (PET).

Keywords: Tumor angiogenesis, molecular imaging, integrin $\alpha_v\beta_3$, RGD peptide, positron emission tomography (PET).

TUMOR ANGIOGENESIS

Angiogenesis, the formation of new blood vessels from preexisting vasculature, is essential for tumor growth and progression (for a review, see ref. [1]). Without neovascularization, cells in prevascular tumors or metastases that may be replicating rapidly reach equilibrium with their rate of death. Inhibition of angiogenesis has been shown to prevent tumor growth and even to cause tumor regression in various experimental models [2]. In contrast to traditional chemotherapies, which non-specifically target all dividing cells, anti-angiogenic therapy selectively targets activated endothelial cells and tumor cells. In early Phase I/II clinical trials, angiogenic modulators have shown modest toxic effects and are mainly cytostatic, slowing or stopping the tumor growth and the development of metastasis, producing an objective remission [3] (see http://www.angiogenesis.org or http://cancernet.nci.nih.gov for a detailed list of agents in development).

Angiogenesis is a complex process involving extensive interplay between cells, soluble factors, and extracellular matrix (ECM) components [1]. The construction of a vascular network requires different sequential steps including the release of proteases from "activated" endothelial cells with subsequent degradation of basement membrane surrounding the existing vessel, migration of endothelial cells into the interstitial space, endothelial cell proliferation, and differentiation into mature blood vessels. These processes are mediated by a wide range of angiogenic inducers, including growth factors, chemokines, angiogenic enzymes, endothelial specific receptors, and adhesion molecules [4]. Each of these processes presents the possible targets for possible diagnostic and therapeutic interventions.

*Address correspondence to this author at the Xiaoyuan Chen, PhD, Molecular Imaging Program at Stanford (MIPS), Department of Radiology, Stanford University, 1201 Welch Rd P095, Stanford, CA 94305-5484, USA; Tel: 650)725-0950; Fax: 650)736-7925; E-mail: shawchen@stanford.edu

ANATOMICAL/FUNCTIONAL IMAGING OF TUMOR ANGIOGENESIS

Because tumor size monitoring is still an important clinical indicator for oncologists, conventional imaging techniques will likely remain useful to follow anti-angiogenic treatment efficacy. These techniques can also be adapted to visualize and quantify morphological and functional changes associated with tumor vascularity. Computed tomography (CT) imaging can be performed with contrast agents to define the intravascular compartment, including blood flow, blood volume, mean fluid transit time, and capillary permeability [5]. Perfusion CT technique can be easily incorporated into the existing CT protocols to delineate increases in tissue perfusion that may reflect malignancy, even when there is no gross anatomical abnormality present [6]. Depiction and detection of tumor vascularity with ultrasound can be either approached by Doppler studies to delineate large and medium-sized vessels or by microbubble contrast enhanced agents to detect microvascularity [7]. Magnetic resonance imaging (MRI) can define both blood volume and blood vessel permeability using dynamic enhancement of blood pool contrast agents. Gadolinium-DTPA can distinguish between normal (non-leaky) versus malignant (leaky) tissues, reflecting the hyperpermeable tumor vasculature. Dynamic MRI used in combination with macromolecular contrast media and kinetic modeling can be applied to monitor changes in the tumor microvasculature such as transendothelial permeability or fractional plasma volume [8,9]. Positron emission tomography (PET) is another approach used to characterize neoplastic tissue. Fluorodeoxyglucose (FDG) labeled with positron emitter ^{18}F ($t_{1/2}$ = 109.7 min) can be used to localize primary tumors and distal metastases and to characterize tumor glucose metabolism [10]. Blood flow and blood volume can also be detected with $H_2{}^{15}O$ and ^{11}CO, respectively [11].

1389-5575/06 $50.00+.00

MOLECULAR IMAGING OF TUMOR INTEGRIN EXPRESSION

Targeting tumor angiogenesis by conventional imaging modalities that detect anatomical and functional changes of tumor vascularity during tumor growth, angiogenesis, and upon anti-angiogenic treatment have been well-documented. These approaches, however, provide little or no information regarding the specific molecular markers on newly formed blood vessels and tumor cells and the molecular changes upon therapy. The evolution of molecular imaging [12,13] takes advantage of traditional diagnostic imaging techniques and introduces molecular imaging probes to determine the expression of indicative molecular markers of the tumor angiogenesis process [14,15] (A detailed depiction of molecular imaging probe development is illustrated in Fig. **1**).

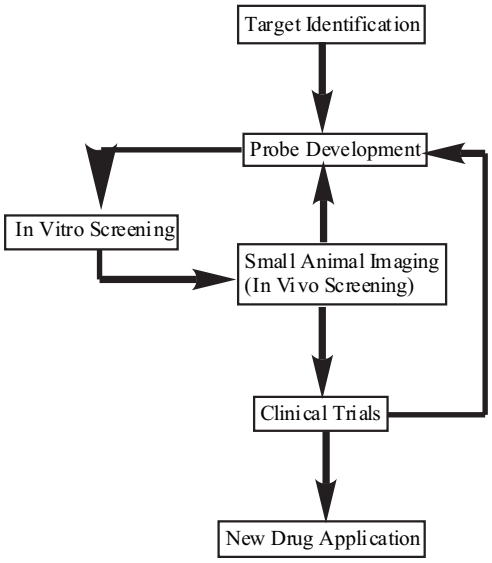

Fig. (1). Molecular Imaging is a novel multidisciplinary field involving the efforts from molecular and cell biology to identify the molecular imaging target, radiochemistry and bioconjugation chemistry to develop suitable imaging probes, pharmacology to optimize the probes for optimal targeting efficacy and favorable *in vivo* kinetics, and signal capture/image reconstruction techniques to non-invasively monitor the fate of molecular imaging probes *in vivo*. Once a molecular imaging target (mRNA or protein) is identified and validated (the target is required to have unique expression on the tumor cells as compared to normal organs and tissues and enough number of copies to be detectable by molecular imaging devices and to provide enough tumor/background contrast), effort will then be spent to develop molecular imaging probes for test (a more detailed description for molecular imaging probe development is shown in (Fig. **2**). The probe will then be applied to preclinical animal models for lesion detection (typically microPET or microSPECT). The tumor targeting efficacy and *in vivo* kinetics will determine whether the probe will be further evaluated. If small animal imaging demonstrates that the molecular probe has good target specific tumor uptake and favorable *in vivo* kinetic profiles, the probe will then be rapidly translated into clinical applications since the features of miniaturized small animal imaging studies closely reflect the settings of a clinical imaging study for human beings. Satisfactory clinical trials for the New Investigational Drug (IND) will enable the submission of New Drug Application (NDA) to the Division of Medical Imaging and Radiopharmaceutical Drug Research, FDA for approval. If the probe fails to provide high tumor-to-background ratio, further structure-activity relationship (SAR) studies will be performed to optimize the molecular imaging probes.

For a targeting approach aimed at monitoring tumor angiogenesis, the accessible targets that are specific for the tumor present at a sufficient level are a prerequisite for the lesion to be detectable and to be delineated from the background by imaging technologies. The cell adhesion molecule integrin $\alpha_v\beta_3$ [16], which is over-expressed on both tumor cells and tumor vasculature, is an excellent molecular marker for tumor angiogenesis imaging. Interactions between vascular cells and extracellular matrixes (ECMs) are involved in the multiple steps of angiogenesis. To date, four families of cell adhesion molecules have been described: integrins, immunoglobulin superfamily members, cadherins, and selectins. Members of each family have been detected in angiogenic blood vessels, with integrins being most well-studied. Adhesion receptors of the integrin family are responsible for a wide range of cell-ECM and cell-cell interactions. Each integrin consists of non-covalently associated α and β subunits, both type I membrane proteins with large extracellular segments that pair to create heterodimers ($\alpha\beta$) with distinct adhesive capabilities. In mammals, 18 α and 8 β subunits assemble into 24 different receptors. The function of integrins during angiogenesis has been studied most extensively with $\alpha_v\beta_3$, which is not readily detectable in quiescent vessels but becomes highly expressed in angiogenic vessels [17]. The expression of integrin adhesion molecule $\alpha_v\beta_3$ on sprouting capillary cells and their interaction with specific matrix ligands has been shown to play a key role in angiogenesis and metastasis. Integrins expressed on endothelial cells modulate cell migration and survival during angiogenesis. Integrins expressed on carcinoma cells potentiate metastasis by facilitating invasion and movement across blood vessels. Inhibition of α_v integrin activity by mAbs, cyclic RGD peptide antagonists, and peptidomimetics has been shown to induce endothelial apoptosis, to inhibit angiogenesis, and to increase endothelial monolayer permeability [18].

The ability to non-invasively visualize and quantify $\alpha_v\beta_3$ integrin expression level will provide new opportunities to document tumor (tumor cells and sprouting tumor vasculature) receptor expression, more appropriately select patients considered for anti-integrin treatment and monitor treatment efficacy in integrin-positive patients (General procedure for molecular imaging probe development is described in (Fig. **2**). Contrast enhanced ultrasound with microbubbles targeted to $\alpha_v\beta$integrins expressed on the neovascular endothelium has been used to image tumor integrin status in addition to tumor microvascular blood volume and blood velocity, which can be easily detected with non-targeted microbubbles [19]. In an animal model, Sipkins *et al.* [20] recently demonstrated that it is feasible to image $\alpha_v\beta_3$ expression using MRI and antibody-coated paramagnetic liposomes. Due to the unfavorable physical characteristics of mAbs (vascularization requirements, and barriers to antibody penetration, as well as intratumoral pressure) and low sensitivity of MRI, targeted MR imaging

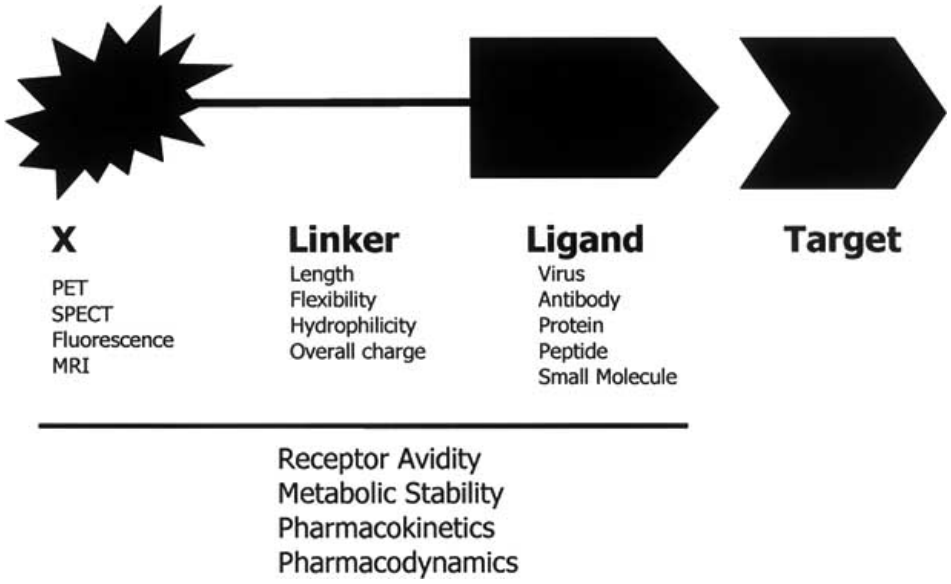

Fig. (2). A molecular imaging probe is often comprised of three parts: the target delivery vehicle (virus particles, monoclonal antibody, bispecific antibody or antibody fragments, proteins, peptides, or small molecule agonists/antagonists), the moiety (radionuclides for PET or SPECT, fluorescent dye for optical imaging or paramagnetic metal ion for MRI) that can be detected by an external imaging device, and a pharmacokinetic modifying (PKM) linker tethering the two together (there are exceptions if a PKM linker is not present, for example, isotopic substitution of a small molecule drug). Even though a target is validated, several factors are yet to be defined to determine whether a molecular imaging probe can be successfully applied for visualization and efficient quantification of the target, namely, receptor binding affinity and specificity, hydrophilicity, metabolic stability, overall molecular charge, molecular size, and the fate of metabolites.

will face significant obstacles to provide a robust platform for tumor integrin assessment. We and others [21,22] have also shown that near-infrared fluorescent dye conjugated cyclic RGD peptide was able to visualize subcutaneously inoculated integrin positive tumors. The major drawback of this approach is the limited penetration of light through tissue that this modality has primarily been directed towards near surface lesions that are accessible by light. Even though optical imaging may not be easily translated into human studies, this approach provides opportunities for rapid and cost-effective preclinical evaluation in animal models before the more costly radionuclide-based imaging studies. To date, most of the studies have been focused on developing suitably radiolabeled small RGD peptide antagonists of α_v-integrin as radiopharmaceuticals for single-photon emission computed tomography (SPECT) and positron emission tomography (PET) imaging applications [23]. Due to the higher sensitivity of PET (10^{-11} – 10^{-12} M) as compared with SPECT (10^{-9}-10^{-10} M), the acquisition of higher count statistics is particularly valuable for detecting the fewest possible cells per unit volume with the least amount of radioactivity [24], development of probes for PET imaging of integrin expression has been the mainstay of the continued effort.

PET IMAGING OF TUMOR INTEGRIN $\alpha_V\beta_3$

The crystal structures of extracellular segment of $\alpha_v\beta_3$ and its complex with a potent cyclic RGD peptide, c(RGDf[NMe]V) (Cilengitide, Merck, Inc., currently under Phase II clinical trials for patients with glioblastoma multiforme who have failed first-line chemotherapy) indicate that RGD binding site of the $\alpha_v\beta_3$ integrin is located in the deep cleft between the two subunits [25,26]. The essential arginine-glycine-aspartic acid (RGD) sequence in this specific bent conformation is desirable for high affinity and specific binding of the peptide ligand with integrin $\alpha_v\beta_3$. Substitution of the amino acid in position 4 (D-Phe in lead structure) with tyrosine allows electrophilic radiohalogenation (e.g., ^{123}I, ^{124}I, ^{125}I, and ^{131}I). Replacement of the amino acid in position 5 with lysine offers a further alternative for radiolabeling by derivatization of the side-chain α-amino group. The lead compound c(RGDyK) was thus first labeled with ^{125}I and the tracer revealed high receptor specific tumor uptake in integrin positive tumors but also persistent localization of radioactivity in the kidney region, presumably due to the electrostatic interaction between the positively charged RGD peptide and the negatively charged surface of renal proximal tubular cells [27,28]. Modifying the peptide with a sugar [27,29] or a poly(ethylene glycol) (PEG) [27] moiety increased the hydrophilicity of the lead compound and neutralized the positive charge on the lysine residue. ^{125}I-labeled galacto-RGD or PEGylated RGD thus had rapid blood clearance, substantially lowered renal uptake but also slightly decreased tumor uptake due to decreased receptor binding affinity upon derivatization.

Encouraged by the ability of sugar and poly(ethylene glycol) to improve *in vivo* kinetic profile of cyclic RGD peptides, both peptides were then labeled with ^{18}F through a prosthetic group ((±)-2-[^{18}F]fluoropropionate ([^{18}F]FP) for RGD-containing glycopeptide [30-32] and 4-[^{18}F]fluorobenzoyl ([^{18}F]FB) for PEGylated RGD peptide [33]). Both compounds had fast blood clearance (less than 0.1 % injected dose/gram (%ID/g) tissue was present as early

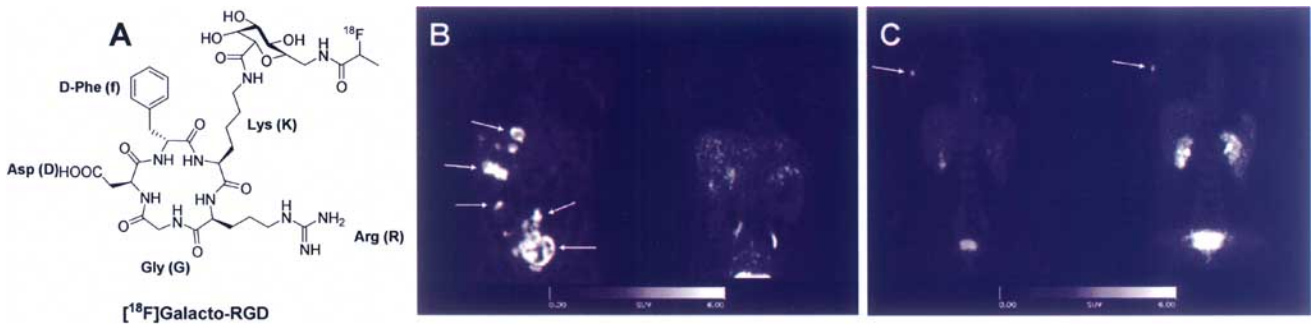

Fig. (3). (A) Schematic structure of [^{18}F]Galacto-RGD. Labeling with (±)-2-[^{18}F]fluoropropionate group was carried out via acylation of the aminomethyl group at the C1-position of the sugar moiety (Adapted from Haubner *et al*., ref. 30). (B) and (C), comparison of [^{18}F]FDG and [^{18}F]Galacto-RGD human scans. (B) A patient with malignant melanoma stage IV and multiple metastases in the liver, skin and lower abdomen (arrows) showed marked uptake of [^{18}F]FDG (left panel) but virtually no uptake of [^{18}F]Galacto-RGD (right panel). (C) A patient with malignant melanoma stage IIIb and a solitary lymph node metastasis in the right axilla can be detected by both [^{18}F]FDG (left panel) and [^{18}F]Galacto-RGD (right panel). The positive [^{18}F]FDG activity accumulation indicates viable tumor cells, whereas specific [^{18}F]Galacto-RGD peptide uptake represents integrin $\alpha_V\beta_3$ positive tumor tissues. Although it is well documented in the literature that the expression of integrin $\alpha_V\beta_3$ is associated with a high risk of metastasis and poor prognosis in melanoma [49], it is not well understood why angiogenesis is observed for the patient with malignant melanoma stage IIIb but not those with malignant stage IV and multiple metastases (Adapted from Haubner *et al*., ref. 32).

as 2 h postinjection of radiotracer), rapid and high tumor uptake and moderate tumor washout, resulting in high tumor-to-background ratio and limited activity accumulation in the liver, kidneys and intestinal tracts. On the other hand, the parent RGD peptide when labeled with ^{18}F through 4-[^{18}F]fluorobenzoyl [34,35], showed tumor specific uptake and its activity accumulation is correlative with tumor integrin levels, however, the rapid tumor washout and unfavorable hepatobiliary excretion of this tracer limited its potential clinical applications. Pilot clinical trials are currently in progress to test the safety and efficacy of ^{18}F-labeled glycosylated RGD monomer and to measure patient integrin expression levels [32] (Fig. **3**).

The low molecular mass compound c(RGDyK) is optimized in size to fit the binding pocket of the $\alpha_v\beta_3$ integrin receptor, thus introduction of any functional group to improve the *in vivo* kinetics is at the expense of a loss of receptor affinity. It has been proposed by several groups that the receptor binding characteristics of dimeric and multimeric RGD peptides would be better than that of monomeric RGD peptide based upon polyvalency [34,36-38]. The receptor binding of the one RGD peptide will significantly enhance the local concentration of the other RGD peptide in the vicinity of the receptor, which may lead to a faster rate of receptor binding or a slower rate dissociation of the radiolabeled dimeric RGD peptide. The dimeric RGD peptide with almost one order of magnitude higher integrin binding affinity than the monomeric analog is thus labeled with ^{18}F [34, 38] and the tracer gave the highest tumor specific activity accumulation and tumor/background ratios at all time points examined as compared to monomeric RGD peptide tracers (unmodified [34,35], PEGylated [33], and glycosylated [34,36-38] RGDs) (Fig. **4**).

For PET imaging of $\alpha_v\beta_3$ expression, ^{18}F-labeled RGD peptides will be the first choice since [^{18}F]F$^-$ is readily available from most medical cyclotron facilities and radiolabeling of peptides with ^{18}F can be realized by introducing a prosthetic group. In addition to ^{18}F, ^{64}Cu-labeled RGD peptides are of considerable interest because ^{64}Cu ($t_{1/2}$ = 12.8 h; β^+ = 655 keV [19%]; β^- = 573 keV [40%]) is an attractive radionuclide for both PET imaging and targeted radiotherapy of cancer [39]. PET imaging of tumors with low doses of ^{64}Cu-labeled RGD peptides could also be utilized to determine individual radiation dosimetry prior to therapy with either ^{64}Cu- or ^{67}Cu-labeled RGD peptides. ^{64}Cu labeling is also fairly straightforward and amenable for kit formulation. Further examples of PET imaging/internal radiotherapy radionuclide pairs include ^{86}Y/^{90}Y [40] and ^{124}I/^{131}I [41].

Generally speaking, the major problems with radiometal labeled peptides for tumor therapy include their rapid blood clearance thus not enough radiation dose being delivered to the tumor and unfavorable non-specific accumulation in non-tumor organs [42]. We initially coupled monomeric RGD peptide c(RGDyK) with macrocyclic chelator 1,4,7,10-tetraazacyclododecane-N,N',N'',N'''-tetraacetic acid (DOTA) and labeled the DOTA-RGD conjugate with ^{64}Cu for breast cancer imaging [43]. The radiotracer showed intermediate tumor uptake but also prominent liver and kidney retention, suggesting both renal and hepatobiliary excretion routes. PEGylated monomeric RGD peptide when labeled with ^{64}Cu, showed significantly reduced liver and intestinal uptake, reflecting favorable renal excretion of this tracer, with tumor targeting efficacy virtually unchanged [44]. A dimeric RGD peptide E[c(RGDyK)]$_2$ with higher integrin binding affinity when labeled with ^{64}Cu indicated almost twice as high uptake in the tumor than the monomeric

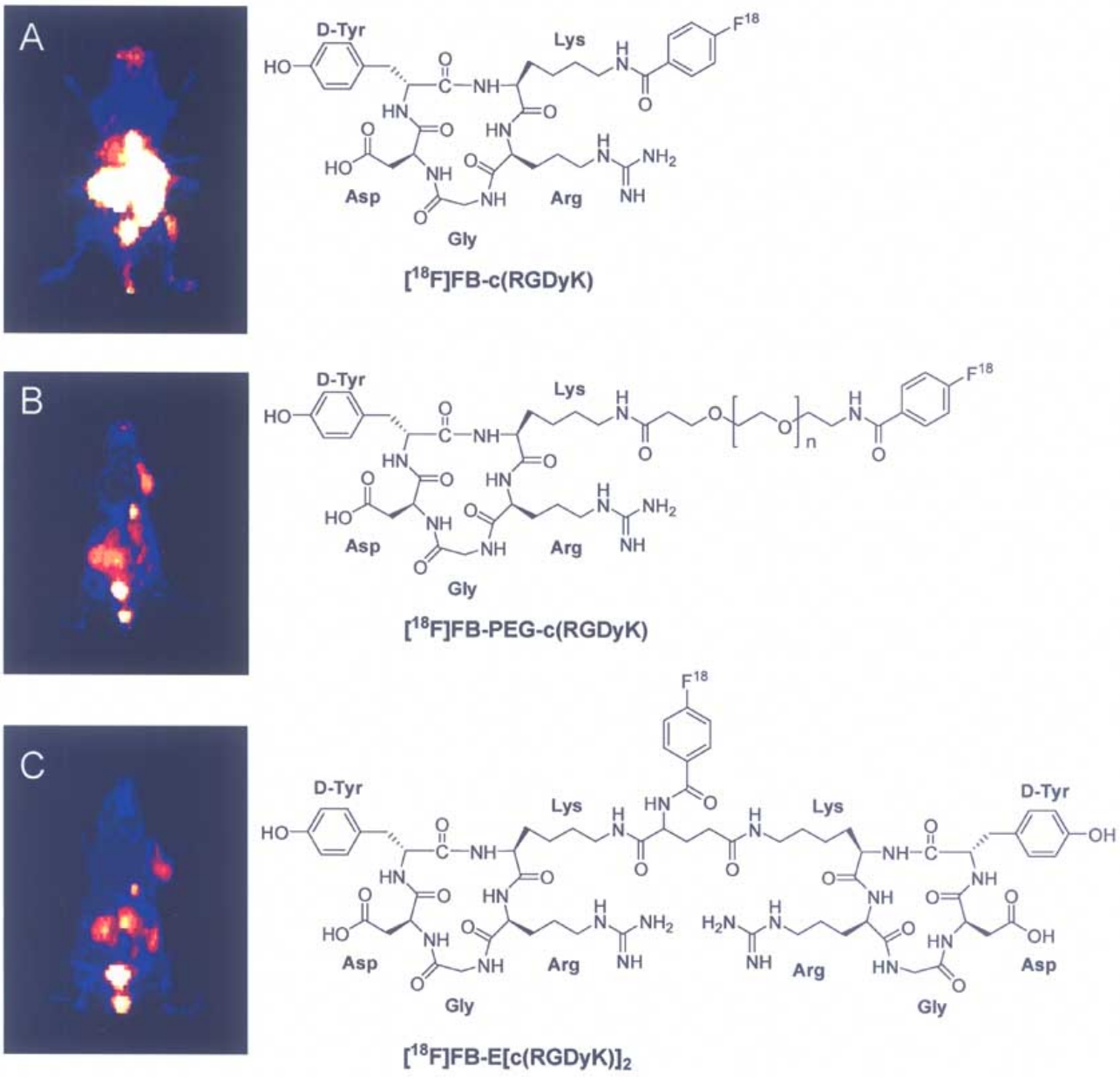

Fig. (4). This figure illustrates how a clinically applicable probe can be developed after identification of integrin $\alpha_V\beta_3$ as the potential target for tumor angiogenesis imaging. Although, the initial compound [^{18}F]FB-c(RGDyK) had a reasonably good receptor binding *in vitro* and tumor specific uptake *in vivo*, it had very rapid tumor washout and unfavorable hepatobiliary excretion, which makes detection of lesions in the lower abdomen very difficult. To increase the water solubility, a poly(ethylene glycol) (M.W. = 3,400) moiety as PKM linker was used to modify the tracer for *in vivo* evaluation. Indeed, the more hydrophilic tracers revealed better *in vivo* profile without compromising the tumor targeting efficacy *in vivo* even although the receptor binding affinity *in vitro* was lowered due to the PEGylation. A dimeric RGD peptide with higher binding affinity, molecular size and hydrophilicity was also labeled with ^{18}F, the tumor uptake was almost twice as much as that of monomeric RGD peptide tracers, and the magnitude of tumor uptake was also positively correlated with tumor integrin density levels as examined in different tumor models. Two-dimensional (2D) projection images were acquired as 10 min static scans 60 min postinjection of 200 μCi of ^{18}F-labeled RGD peptide tracer and reconstructed with ordered subset expectation maximization (OSEM) algorithm using microPET R4 system (Concorde Microsystems, Inc.).

analog, but also significantly higher renal activity accumulation presumably due to the fact that the dimeric RGD peptide tracer is more positively charged than the monomeric counterpart [34,37]. A tetrameric RGD peptide $E\{E[c(RGDyK)]_2\}_2$ with even higher receptor affinity than the dimeric RDG peptide $E[c(RGDyK)]_2$ was labeled with ^{64}Cu and applied to subcutaneous U87MG glioma model and found that the tracer had rapid liver and renal clearance, high and persistent tumor activity accumulation (e.g. tumor uptake was as high as 13 %ID/g at 2 h postinjection). This tracer may have the properties suitable for integrin targeted internal radiotherapeutic applications [45].

FUTURE OUTLOOK

Up to now, most studies for imaging integrin receptor, a key player in tumor angiogenesis is still at the stage of imaging probe development. Systematic structure-activity relationship (SAR) studies are still needed to optimize the probes for optimal tumor targeting efficacy and improved *in vivo* kinetics for clinical trials. Furthermore, little has been done to correlate the magnitude of tumor uptake (combined receptor specific activity accumulation in the tumor cells and tumor vasculature) with integrin expression level. In other words, is the contrast obtained from non-invasive imaging a true reflection of tumor integrin levels? At any given time, the *in vivo* tumor signal is not only due to specific binding, but it also presents contributions from non-specific binding, free imaging probe in tissue, and intravascular activity. Tumor binding potential may be quantified through kinetic modeling of the dynamic microPET imaging data [46,47] and correlated with tumor integrin expression levels examined by traditional histopathological means.

Molecular imaging of tumor angiogenesis targeting at cell adhesion molecule integrin $\alpha_v\beta_3$ may be designed to address the following aims (a schematic plot of the role of integrin expression imaging is illustrated in Fig. **5**):

1). Lesion Detection

In spite of the clinical success with PET, [^{18}F]FDG PET imaging has several limitations. The tracer can be non-specifically taken up by several benign conditions such as inflammatory disease, pneumonia, brown fat, muscle, bowel uptake, and granulomatous disease. Also, slow growing indolent tumors may exhibit only mildly increased glucose metabolism and therefore be missed by FDG PET [10]. As most tumor vasculature endothelial cells and many tumor cells express integrin $\alpha_v\beta_3$, suitably labeled RGD peptides might be a potentially more advantageous surrogate marker than FDG for early detection of some cancer types.

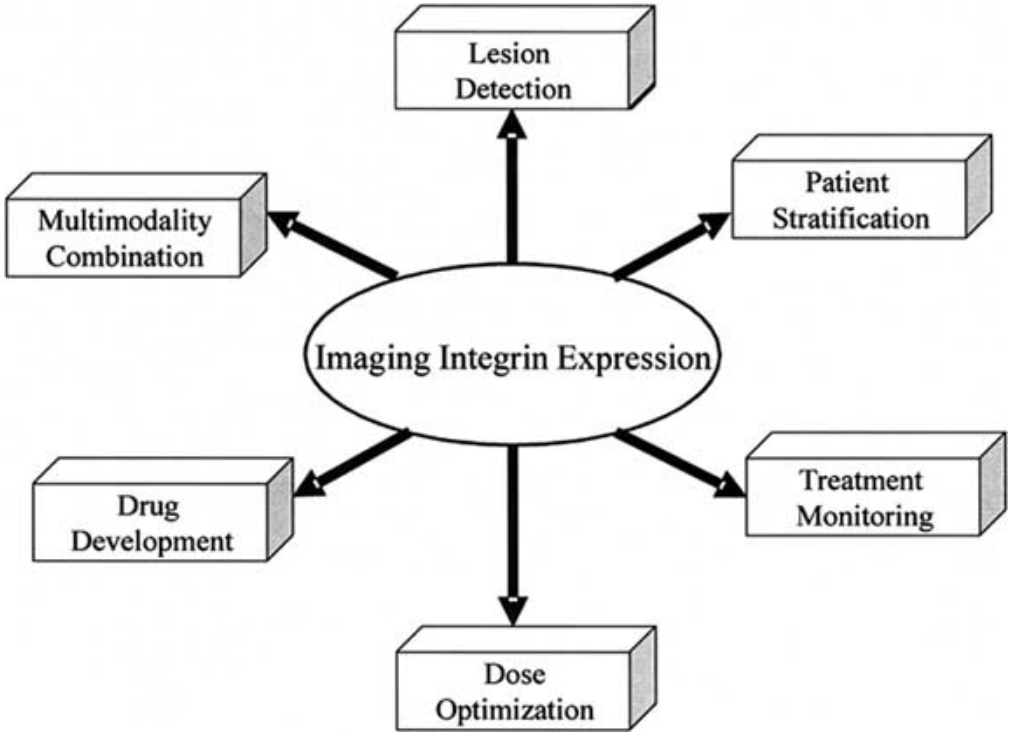

Fig. (5). Molecular imaging of tumor integrin expression may provide new insights into the mechanism of tumor angiogenesis and anti-angiogenic treatment efficacy in addition to simple lesion detection. RGD peptide based PET tracers are expected to supersede FDG for slowing growing tumors such as prostate cancer that exhibit only slightly increased glucose metabolism but have overexpressed integrin expression on both cells and tumor vessels. Quantitative visualization of tumor integrin can be used for patient stratification to accurately document $\alpha_v\beta_3$ levels, this provides evidence for selecting appropriate patients into clinical trials for personalized anti-integrin treatment and to follow treatment efficacy. Receptor occupancy studies may also aid in dosage and dose interval selection for tailored dose optimization. Optimized probes for integrin imaging purpose may be easily adapted to develop new drugs for better tumor localization and retention with minimal non-specific accumulation. The same principle for integrin-based molecular imaging is applicable to molecular imaging in general.

2). Patient Stratification

It is anticipated that there will be great variance in tracer accumulation in different tumor types, which indicates a great diversity in integrin receptor expression. This will indicate the importance of quantitative imaging of tumor integrin for patient stratification, allowing for appropriate selection of integrin positive patients entering clinical trials for anti-integrin treatment.

3). Treatment

Monitoring. The intrinsic redundancy of signaling mechanisms associated with angiogenesis will lead to partial or complete resistance of the tumor vessel to therapy. Non-invasive visualization and quantification of tumor integrin levels may be applied to detect early response to anti-integrin treatment and help to elucidate the mechanisms of treatment efficacy underlying integrin signaling.

4). Dose Optimization

Using an established PET tracer for α_v-integrin receptor expression imaging, one can expect to measure the degree to which administration of a peptide or antibody based integrin antagonist compete with the radiotracer/integrin binding. By this means, one can determine receptor binding potential as well as the percentage of receptor occupancy by administered drug when given in various doses and routes of administration. Furthermore, receptor occupancy studies as a function time after drug administration can be used to establish a favorable dosing interval for the cytostatic drug.

5). New Drug Development/Validation

In vitro receptor binding affinity and specificity may not directly reflect *in vivo* tumor receptor occupancy due to the *in vivo* effects on binding kinetics. PET imaging in combination with radiolabeled RGD peptides might be a useful tool for studying structure-activity relationships for new anti-integrin drugs. Rapid characterization of pharmacokinetics and pharmacodynamics by *in vivo* imaging will inevitably improve data quality, reduce costs and animal numbers used and, most importantly, decrease the work-up for new compounds. The studies with microPET can be directly translated into clinical PET since the features of small animal PET imaging studies closely reflect the settings of clinical PET study for human beings.

6). Combination of Molecular and Functional Imaging

The combination of molecular and anatomical/functional imaging techniques in assessing tumor angiogenesis and in response to anti-angiogenic based therapy will be a powerful tool. Whereas anatomical/functional imaging with better resolution is aimed at identification of a tumoral mass and the assessment of its size and vascularization, PET imaging of integrin expression is better suited for receptor characterization. A multi-modality approach for tumor angiogenesis imaging is therefore the best strategy. The new generation clinical PET-CT [48] will facilitate this by allowing simultaneous PET and CT studies which may be difficult or even impossible with either imaging modality alone.

Tumor integrin expression imaging is given as an example here to demonstrate how molecular imaging can provide a robust platform for the understanding of mechanisms of tumor angiogensis and for the evaluation of novel anti-angiogenic and proangiogenic therapies. Questions remain on how to improve the sensitivity and resolution of molecular imaging technologies and to develop optimal molecular imaging probes as surrogate markers to pinpoint and monitor specific molecular and cellular actions of angiogenesis inhibitors. Whether the magnitude of tracer accumulation is a true reflection of integrin $\alpha_v\beta_3$ expression remains unclear and needs to be developed. The combination and/or fusion of anatomical/functional/molecular imaging techniques will be involved to make this happen.

ACKNOWLEDGMENTS

The author thanks Dr. Sanjiv Sam Gambhir for very helpful discussions and critical manuscript review. Supported, in part, by National Institute of Biomedical Imaging and Bioengineering (NIBIB) Grant R21 EB001785, Department of Defense (DOD) Breast Cancer Research Program (BCRP) Concept Award DAMD17-03-1-0752, DOD BCRP IDEA Award W81XWH-04-1-0697, DOD Prostate Cancer Research Program (PCRP) New Investigator Award (NIA) DAMD1717-03-1-0143, American Lung Association California (ALAC), the Society of Nuclear Medicine Education and Research Foundation, National Cancer Institute (NCI) Small Animal Imaging Resource Program (SAIRP) grant R24 CA93862, and NCI *In Vivo* Cellular Molecular Imaging Center (ICMIC) grant P50 CA114747.

REFERENCES

[1] Bergers, G.; Benjamin, L. E. *Nat. Rev. Cancer,* **2003,** *3*, 401-10.
[2] Siemann, D. W.; Chaplin, D. J.; Horsman, M. R. *Cancer,* **2004,** *100*, 2491-9.
[3] Brower, V. *Nat. Biotechnol.,* **1999,** *17*, 963-8.
[4] Jung, Y. D.; Ahmad, S. A.; Liu, W.; Reinmuth, N.; Parikh, A.; Stoeltzing, O.; Fan, F.; Ellis, L. M. *Semin. Cancer Biol.,* **2002,** *12*, 105-12.
[5] Lee, T. Y.; Purdie, T. G.; Stewart, E. *Q. J. Nucl. Med.,* **2003,** *47*, 171-87.
[6] Miles, K. A. *Br. J. Radiol.,* **2003,** *76*, S36-42.
[7] Cosgrove, D. *Br. J. Radiol.* **2003,** *76*, S43-9.
[8] Abu-Hajir, M.; Rand, S. D.; Krouwer, H. G.; Schmainda, K. M. *Semin. Thromb. Hemost.,* **2003,** *29*, 309-15.
[9] Turetschek, K.; Preda, A.; Novikov, V.; Brasch, R. C.; Weinmann, H. J.; Wunderbaldinger, P.; Roberts, T. P. *J. Magn. Reson. Imaging,* **2004,** *20*, 138-44.
[10] Gambhir, S. S.; Czernin, J.; Schwimmer, J.; Silverman, D. H.; Coleman, R. E.; Phelps, M. E. *J. Nucl. Med.,* **2001,** *42*, 1S-93S.
[11] Laking, G. R.; Price, P. M. *Br. J. Radiol.,* **2003,** *76*, S50-9.
[12] Gambhir, S. S. *Nat. Rev. Cancer,* **2002,** *2*, 683-93.
[13] Massoud, T. F.; Gambhir, S. S. *Genes Dev.,* **2003,** *17*, 545-80.
[14] McDonald, D. M.; Choyke, P. L. *Nat. Med.,* **2003,** *9*, 713-25.
[15] Schirner, M.; Menrad, A.; Stephens, A.; Frenzel, T.; Hauff, P.; Licha, K. *Ann. N. Y. Acad. Sci.,* **2004,** *1014*, 67-75.
[16] Hynes, R. O. *Nat. Med.,* **2002,** *8*, 918-21.
[17] Brooks, P. C.; Clark, R. A.; Cheresh, D. A. *Science,* **1994,** *264*, 569-71.
[18] Tucker, G. C. *Curr. Opin. Investig. Drugs,* **2003,** *4*, 722-31.
[19] Ellegala, D. B.; Leong-Poi, H.; Carpenter, J. E.; Klibanov, A. L.; Kaul, S.; Shaffrey, M. E.; Sklenar, J.; Lindner, J. R. *Circulation,* **2003,** *108*, 336-41.

[20] Sipkins, D. A.; Cheresh, D. A.; Kazemi, M. R.; Nevin, L. M.; Bednarski, M. D.; Li, K. C. *Nat. Med.,* **1998,** *4*, 623-6.
[21] Chen, X.; Conti, P. S.; Moats, R. A. *Cancer Res.,* **2004,** *64*, 8009-14.
[22] Wang, W.; Ke, S.; Wu, Q.; Charnsangavej, C.; Gurfinkel, M.; Gelovani, J. G.; Abbruzzese, J. L.; Sevick-Muraca, E. M.; Li, C. *Mol. Imaging,* **2004,** *3*, 343-51.
[23] Haubner, R.; Wester, H. J. *Curr. Pharm. Des.,* **2004,** *10*, 1439-55.
[24] Wu, A. M.; Yazaki, P. J.; Tsai, S.; Nguyen, K.; Anderson, A. L.; McCarthy, D. W.; Welch, M. J.; Shively, J. E.; Williams, L. E.; Raubitschek, A. A.; Wong, J. Y.; Toyokuni, T.; Phelps, M. E.; Gambhir, S. S. *Proc. Natl. Acad. Sci. U. S. A.,* **2000,** *97*, 8495-500.
[25] Xiong, J. P.; Stehle, T.; Zhang, R.; Joachimiak, A.; Frech, M.; Goodman, S. L.; Arnaout, M. A. *Science,* **2002,** *296*, 151-5.
[26] Gottschalk, K. E.; Kessler, H. *Angew. Chem. Int. Ed. Engl.,* **2002,** *41*, 3767-74.
[27] Chen, X.; Park, R.; Shahinian, A. H.; Bading, J. R.; Conti, P. S. *Nucl. Med. Biol.,* **2004,** *31*, 11-9.
[28] Haubner, R.; Wester, H. J.; Reuning, U.; Senekowitsch-Schmidtke, R.; Diefenbach, B.; Kessler, H.; Stocklin, G.; Schwaiger, M. *J. Nucl. Med.,* **1999,** *40*, 1061-71.
[29] Haubner, R.; Wester, H. J.; Burkhart, F.; Senekowitsch-Schmidtke, R.; Weber, W.; Goodman, S. L.; Kessler, H.; Schwaiger, M. *J. Nucl. Med.,* **2001,** *42*, 326-36.
[30] Haubner, R.; Wester, H. J.; Weber, W. A.; Mang, C.; Ziegler, S. I.; Goodman, S. L.; Senekowitsch-Schmidtke, R.; Kessler, H.; Schwaiger, M. *Cancer Res.,* **2001,** *61*, 1781-5.
[31] Haubner, R.; Kuhnast, B.; Mang, C.; Weber, W. A.; Kessler, H.; Wester, H. J.; Schwaiger, M. *Bioconjug. Chem.,* **2004,** *15*, 61-9.
[32] Haubner, R.; Weber, W. A.; Beer, A. J.; Vabuliene, E.; Reim, D.; Sarbia, M.; Becker, K. F.; Goebel, M.; Hein, R.; Wester, H. J.; Kessler, H.; Schwaiger, M. *PLoS Med.,* **2005,** *2*, e70.
[33] Chen, X.; Park, R.; Hou, Y.; Khankaldyyan, V.; Gonzales-Gomez, I.; Tohme, M.; Bading, J. R.; Laug, W. E.; Conti, P. S. *Eur. J. Nucl. Med. Mol. Imaging,* **2004,** *31*, 1081-9.
[34] Chen, X.; Liu, S.; Hou, Y.; Tohme, M.; Park, R.; Bading, J. R.; Conti, P. S. *Mol. Imaging Biol.,* **2004,** *6*, 350-9.
[35] Chen, X.; Park, R.; Shahinian, A. H.; Tohme, M.; Khankaldyyan, V.; Bozorgzadeh, M. H.; Bading, J. R.; Moats, R.; Laug, W. E.; Conti, P. S. *Nucl. Med. Biol.,* **2004,** *31*, 179-89.
[36] Thumshirn, G.; Hersel, U.; Goodman, S. L.; Kessler, H. *Chemistry,* **2003,** *9*, 2717-25.
[37] Chen, X.; Sievers, E.; Hou, Y.; Park, R.; Tohme, M.; Bart, R.; Bremner, R.; Bading, J. R.; Conti, P. S. *Neoplasia,* **2005,** *7*, 271-9.
[38] Chen, X.; Tohme, M.; Park, R.; Hou, Y.; Bading, J. R.; Conti, P. S. *Mol. Imaging,* **2004,** *3*, 96-104.
[39] McCarthy, D. W.; Shefer, R. E.; Klinkowstein, R. E.; Bass, L. A.; Margeneau, W. H.; Cutler, C. S.; Anderson, C. J.; Welch, M. J. *Nucl. Med. Biol.,* **1997,** *24*, 35-43.
[40] Helisch, A.; Forster, G. J.; Reber, H.; Buchholz, H. G.; Arnold, R.; Goke, B.; Weber, M. M.; Wiedenmann, B.; Pauwels, S.; Haus, U.; Bouterfa, H.; Bartenstein, P. *Eur. J. Nucl. Med. Mol. Imaging,* **2004,** *31*, 1386-92.
[41] Verel, I.; Visser, G. W.; Vosjan, M. J.; Finn, R.; Boellaard, R.; van Dongen, G. A. *Eur. J. Nucl. Med. Mol. Imaging,* **2004,** *31*, 1645-52.
[42] Kwekkeboom, D.; Krenning, E. P.; de Jong, M. *J. Nucl. Med.,* **2000,** *41*, 1704-13.
[43] Chen, X.; Park, R.; Tohme, M.; Shahinian, A. H.; Bading, J. R.; Conti, P. S. *Bioconjug. Chem.,* **2004,** *15*, 41-9.
[44] Chen, X.; Hou, Y.; Tohme, M.; Park, R.; Khankaldyyan, V.; Gonzales-Gomez, I.; Bading, J. R.; Laug, W. E.; Conti, P. S. *J. Nucl. Med.,* **2004,** *45*, 1776-83.
[45] Wu, Y.; Fisher, D. R.; Liu, S.; Chen, X. *J. Nucl. Med.,* **2005,** *46*, 27P.
[46] Schmidt, K. C.; Turkheimer, F. E. *Q. J. Nucl. Med.,* **2002,** *46*, 70-85.
[47] Logan, J. *Nucl. Med. Biol.,* **2000,** *27*, 661-70.
[48] Kapoor, V.; McCook, B. M.; Torok, F. S. *Radiographics,* **2004,** *24*, 523-43.
[49] Kageshita, T.; Hamby, C. V.; Hirai, S.; Kimura, T.; Ono, T.; Ferrone, S. *Int. J. Cancer,* **2000,** *89*, 153-9.

Received: April 29, 2005 Revised: June 02, 2005 Accepted: June 03, 2005